
Propagation of elastic waves through polycrystals: the effects of scattering from dislocation arrays

BY AGNÈS MAUREL^{1,*}, VINCENT PAGNEUX², DENIS BOYER³
AND FERNANDO LUND^{4,5}

¹*Laboratoire Ondes et Acoustique, UMR CNRS 7587, Ecole Supérieure de Physique et de Chimie Industrielles, 10 rue Vauquelin, 75005 Paris, France*

²*Laboratoire d'Acoustique de l'Université du Maine, UMR CNRS 6613, Av. Olivier Messiaen, 72085 Le Mans Cedex 9, France*

³*Instituto de Física, Universidad Nacional Autónoma de México, Apartado Postal 20-364, 01000 México D.F., México*

⁴*Departamento de Física, Facultad de Ciencias Físicas y Matemáticas, Universidad de Chile, Casilla 487-3, Santiago, Chile*

⁵*Centro para la Investigación Interdisciplinaria Avanzada en Ciencias de los Materiales (CIMAT), Casilla 487-3, Santiago, Chile*

We address the problem of an elastic wave coherently propagating through a two-dimensional polycrystal. The main source of scattering is taken to be the interaction with grain boundaries that are in turn modelled as line distribution of dislocations—a good approximation for low angle grain boundaries. First, the scattering due to a single linear array is worked out in detail in a Born approximation, both for longitudinal and transverse polarization and allowing for mode conversion. Next, the polycrystal is modelled as a continuum medium filled with such lines that are in turn assumed to be randomly distributed. The properties of the coherent wave are worked out in a multiple scattering formalism, with the calculation of a mass operator, the main technical ingredient. Expansion of this operator to second-order in perturbation theory gives expressions for the index of refraction and attenuation length. This work is motivated by two sources of recent experiments: firstly, the experiments of Zhang *et al.* (Zhang, G., Simpson Jr, W. A., Vitek, J. M., Barnard, D. J., Tweed, L. J. & Foley J. 2004 *J. Acoust. Soc. Am.* **116**, 109–116.) suggesting that current understanding of wave propagation in polycrystalline material fails to interpret experimental results; secondly, the experiments of Zolotoyabko & Shilo who show that dislocations are potentially strong scatterers for elastic waves.

Keywords: dislocations; grain boundary; polycrystal; scattering function; multiple scattering; effective medium

* Author for correspondence (agnes.maurel@espci.fr).

1. Introduction

The propagation of sound in polycrystals has long been an object of study (for a review see, for instance, [Thompson 2002](#)). Individual grains within a polycrystal are single crystals, each with its own orientation, separated by grain boundaries. While the material within each grain is the same, the orientation of the crystal axes is different and it is this contrast in anisotropy that is at the root of the way elastic waves will behave in a polycrystal. Following the pioneer works of [Lifshitz & Parkhomovskii \(1950\)](#), the general approach to study sound propagation in polycrystals has been to consider a theory in which the elastic constants of the grains fluctuate. Methods include multiple scattering ([Stanke & Kino 1984](#)), use of a second-order Born approximation on an individual scatterer ([Hirsekorn 1982](#)) and geometrical acoustics ([Rokhlin *et al.* 1991](#)). Recent experiments of wave propagation in single phase polycrystalline material ([Zhang *et al.* 2004](#)), however, appear to be quite at variance with current theoretical modelling, thus suggesting a need to revisit the issue of sound elastic wave propagation in polycrystals. At the same time, other experiments ([Zolotoyabko *et al.* 2001](#); [Shilo & Zolotoyabko 2002, 2003](#)) have illustrated that wave scattering by dislocations can be significant.

Low angle grain boundaries are well described as arrays of aligned edge dislocations (see [figure 1](#)). This is why we propose in this paper to address the problem of wave scattering by dislocation segments, a problem that has been disregarded before. To clearly isolate this effect, we do not include in our analysis the scattering coming from the different elastic properties between grains. We only consider the grain boundaries as interfaces able to be the sources of the scattering, while the medium they limit is taken to be the same, namely homogeneous and isotropic.

The interaction between an elastic wave and a dislocation was first analysed by [Eshelby \(1949, 1953\)](#) and [Nabarro \(1951\)](#) by use of an electromagnetic analogy. A different approach has been largely developed by [Granato & Lücke \(Granato & Lücke 1956*a,b*, 1966, 1981; Lücke & Granato 1981\)](#) who model the dislocation as a string driven by a scalar time-dependent stress. [Eshelby & Nabarro](#) noted that the waves are scattered by a dislocation, because their motion induced by the incoming wave generates the emission of a scattered wave. Thus, a description of this mechanism involves two steps: the knowledge of the law of motion of a dislocation in the presence of an incident wave, and a representation for the elastic field generated by the moving dislocation. As an integral representation for the velocity field generated by a moving dislocation was derived from the Navier equations by [Mura](#) in 1963, the general framework to obtain the equations for the motion of a dislocation in the presence of an incident wave is much more recent ([Lund 1988](#)). This is probably why little about the interaction between elastic waves and dislocations can be found in the literature. Very recently, we have tackled this problem in a bi-dimensional configuration. Firstly, we have considered the problem for the interaction between a single dislocation and an elastic wave ([Maurel *et al.* 2004a](#)). Then, we have studied the properties of a coherent wave (its refraction index and attenuation length) propagating in a medium filled with randomly placed dislocations ([Maurel *et al.* 2004b](#)), the motivation being to extend the ultrasonic non-destructive evaluation for the detection of flaws and cracks to the ultrasonic

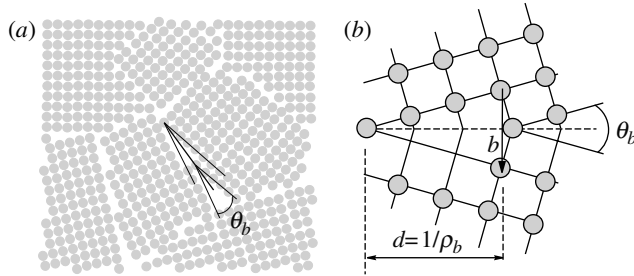


Figure 1. (a) Polycrystalline structure, (b) low angle (tilt) grain boundary and corresponding Burgers vector.

non-destructive evaluation of dislocation ensembles, thus enabling a non-intrusive probe for the study of plasticity.

In this paper, we focus on the two-dimensional multiple scattering process generated by a random distribution of lines that are composed of a line distribution of edge dislocations within an otherwise homogeneous isotropic medium. This is our cartoon of a polycrystal. The paper is organized as follows: in §2, we present the basic relations that lead to an homogeneous wave equation for the in-plane velocity associated with wave displacement,

$$[\nabla^2 + k_\beta^2 + (\gamma^2 - 1)\nabla\nabla.]v(\mathbf{x}) = -\mathbf{V}^{\text{GB}}(\mathbf{x})v(\mathbf{x}). \quad (1.1)$$

Equation (1.1) has a classical form: the left-hand side term corresponds to the usual wave equation whose solutions are two in-plane waves: a transverse wave with a wavevector of modulus k_β , and a longitudinal wave of modulus $k_\alpha = k_\beta/\gamma$. The right-hand side term describes the interaction between the waves and the grain boundary (i.e. the scatterer) through the potential \mathbf{V}^{GB} that has a matrix structure. Then, equation (1.1) is used to determine the scattering functions for a single grain boundary. For in-plane polarized waves, four scattering functions have to be determined. Sections 3 and 4 treat the coherent propagation of waves through multiple grain boundaries (let us remind that these multiple grain boundaries are our cartoon of a polycrystal). In §3, the multiple scattering formalism is presented. Because of the linearity of equation (1.1), the potential \mathbf{V} for a grain boundary ensemble, each grain boundary being indexed by i , is simply deduced from the potential \mathbf{V}^{GB_i} for a single grain boundary through $\mathbf{V} = \sum_i \mathbf{V}^{\text{GB}_i}$. The main task here is to derive the so-called modified, or averaged, Green's function that is the impulse response of the effective medium, defined as the average of the media over all realizations of grain boundary ensembles. In §4, the characteristics of the coherent wave, in terms of velocity and attenuation, are derived and discussed.

We report in the electronic supplementary material some technical algebra.

2. Scattering mechanism

We recall in this section the main results obtained in Maurel *et al.* (2004a) to obtain the potential \mathbf{V}^D for a scatterer composed of a single dislocation. The potential \mathbf{V}^{GB} for a dislocation ensemble is $\mathbf{V}^{\text{GB}} = \int_{\mathcal{L}} dX_i \rho_b(X_i) \mathbf{V}^D$ corresponding

to a line distribution of dislocations with a line density $\rho_b(X_i)$. In the following, we assume this density to be constant [$\rho_b(X_i) = \rho_b$], i.e. we assume the grain boundary is formed of a uniform distribution of dislocations. Note that we could consider \mathbf{V}^{GB} as a discrete sum over point dislocations (i.e. a line density made of delta functions); this latter choice being less tractable mathematically.

We consider a two-dimensional space with the fixed basis $(O, \mathbf{e}_1, \mathbf{e}_2)$. Dislocations are gliding edge dislocations, i.e. their Burgers vectors \mathbf{b} are in-plane and their motion, described by the dislocation position \mathbf{X} , occurs along the Burgers vector \mathbf{b} . The basis attached to the dislocation is (\mathbf{t}, \mathbf{n}) , with $\mathbf{b} = b\mathbf{t}$ and \mathbf{n} along the in-plane perpendicular direction. The two types of in-plane waves interacting with an edge dislocation are: a longitudinal wave with compressional velocity $\alpha = \sqrt{(\lambda + 2\mu)/\rho}$ and a transverse wave with shear velocity $\beta = \sqrt{\mu/\rho}$, where (λ, μ) are Lamé's constants and ρ the density of the elastic medium. We define $\gamma \equiv \alpha/\beta$, as in equation (1.1).

(a) *Potential for a single dislocation*

In this section, we want to obtain the potential for a single dislocation. Firstly, equation (2.1) is the starting relation to do that. It corresponds to the integral representation for the particle velocity $\mathbf{v} \equiv \dot{\mathbf{u}}$ (\mathbf{u} is the displacement field in the elastic medium and the dot denotes the time derivative) produced by a moving dislocation located at position \mathbf{X} . Secondly, equation (2.3) is the equation of motion of a gliding edge dislocation in the presence of an incident wave.

The integral representation

$$v_m(\mathbf{x}, t) = \epsilon_{kn} c_{ijkl} \int dt' b_l \dot{X}_n(t') \frac{\partial}{\partial x_j} \mathbf{G}_{im}^0(\mathbf{x} - \mathbf{X}, t - t'), \quad (2.1)$$

is derived from the wave equation

$$\rho \ddot{u}_i(\mathbf{x}, t) - c_{ijkl} \frac{\partial^2}{\partial x_j \partial x_k} u_l(\mathbf{x}, t) = 0, \quad (2.2)$$

with boundary conditions

$$[u_i]_{S(t)} = b_i, \quad \left[c_{ijkl} \frac{\partial u_l}{\partial x_k} n_j \right]_{S(t)} = 0,$$

where $S(t)$ is a time-dependent line abutting at the dislocation point (in two-dimensional) and the brackets denote the difference above and below $S(t)$. A derivation of the integral representation has been performed in Mura (1963) and is detailed in electronic supplementary material-1. Similar derivation can be found in Lund (2002) for a vortex loop configuration. In equation (2.1), the indexes $j, k, n \dots$ take the value 1 or 2, and $\epsilon_{kn} \equiv \epsilon_{kn3}$ (the usual completely antisymmetric tensor). $\mathbf{G}_{im}^0(\mathbf{x}, t)$ is the elastic Green function in two dimensions.

In the local basis (\mathbf{t}, \mathbf{n}) introduced earlier, the equation of motion for a gliding dislocation reads

$$m \ddot{\mathbf{X}}(t) = \tilde{\sigma}_{12} \mathbf{b}, \quad (2.3)$$

where $\tilde{\sigma}_{12}$ is the stress tensor expressed in the local basis (\mathbf{t}, \mathbf{n}) taken at the position $\mathbf{X}(t)$ of the dislocation and where m is the effective mass of an edge

dislocation

$$m = \frac{1}{4\pi} \frac{1 + \gamma^4}{\gamma^4} \rho b^2 \ln \frac{\delta}{\delta_0}, \quad (2.4)$$

with δ and δ_0 the long- and short-distance cut-off lengths, respectively.

This equation, valid in the subsonic case (dislocation velocity small compared with α, β), corresponds to an edge dislocation with mass m submitted to the usual Peach–Koehler force (Peach & Koehler 1950). For the derivation of this equation, see for instance Lund (1988).

Equations (2.1) and (2.3) can be combined into the following wave equation written in the frequency domain (ω denotes the frequency and $k_\beta \equiv \omega/\beta$)

$$[\nabla^2 + k_\beta^2 + (\gamma^2 - 1)\nabla\nabla\cdot]v(\mathbf{x}) = -\mathbf{V}^D(\mathbf{x})v(\mathbf{x}), \quad (2.5)$$

where the right-hand side of this equation is a two-component vector ‘potential’ given by

$$\mathbf{V}^D(\mathbf{x})v(\mathbf{x}) \equiv \begin{pmatrix} s_t(\mathbf{x}) \\ s_n(\mathbf{x}) \end{pmatrix} = \frac{\mu b^2}{m\omega^2} (\partial_n v_t + \partial_t v_n)|_{\mathbf{X}} \begin{pmatrix} \partial_n \\ \partial_t \end{pmatrix} \delta(\mathbf{x} - \mathbf{X}), \quad (2.6)$$

in the local basis (\mathbf{t}, \mathbf{n}) and with $\partial_a v|_{\mathbf{X}}$ denoting $(\partial v/\partial a)(\mathbf{X})$ (∂_t represents the space derivative along the tangent t , not to be confused with a time derivative (dot symbol)). A detailed derivation of this equation can be found in electronic supplementary material-2.

Introducing the matrix $\mathbf{J} = \begin{pmatrix} 0 & 1 \\ 1 & 0 \end{pmatrix}$, one can express the components $\tilde{\mathbf{V}}^D$ of the operator in the local basis as

$$\begin{pmatrix} s_t(\mathbf{x}) \\ s_n(\mathbf{x}) \end{pmatrix} = -\tilde{\mathbf{V}}^D(\mathbf{x}) \begin{pmatrix} v_t(\mathbf{x}) \\ v_n(\mathbf{x}) \end{pmatrix}, \quad \text{with} \quad \tilde{\mathbf{V}}^D(\mathbf{x}) = \frac{\mu b^2}{m\omega^2} \mathbf{J} \tilde{\nabla} \delta(\mathbf{x} - \mathbf{X}) \tilde{\nabla}|_{\mathbf{X}}^T \mathbf{J},$$

where $\tilde{\nabla} \equiv \begin{pmatrix} \partial_t \\ \partial_n \end{pmatrix}$ and $\tilde{\nabla}|_{\mathbf{X}}^T$ is the operator (acting on any function $f(\mathbf{x})$) defined as

$$\tilde{\nabla}|_{\mathbf{X}}^T f(\mathbf{x}) \equiv \begin{pmatrix} \partial_t f(\mathbf{X}) \\ \partial_n f(\mathbf{X}) \end{pmatrix}. \quad \text{Superscript T denotes the transpose.}$$

Expressing all quantities in the basis $(\mathbf{e}_1, \mathbf{e}_2)$, the operator \mathbf{V}^D finally reads

$$\mathbf{V}^D(\mathbf{x}) = \frac{\mu b^2}{m\omega^2} \mathbf{R}_{2\theta_0} \mathbf{J} \nabla \delta(\mathbf{x} - \mathbf{X}) \nabla|_{\mathbf{X}}^T \mathbf{R}_{2\theta_0} \mathbf{J}, \quad (2.7)$$

with $\theta_0 \equiv \widehat{(\mathbf{e}_1, \mathbf{b})}$ and $\mathbf{R}_a \equiv \begin{pmatrix} \cos a & -\sin a \\ \sin a & \cos a \end{pmatrix}$ the rotation matrix of angle a . We have used $\mathbf{R}_a \mathbf{J} = \mathbf{J} \mathbf{R}_{-a}$.

(b) ‘Potential’ for a grain boundary

A grain boundary is represented by a segment \mathcal{L} of length L , containing $N = \rho_b L$ dislocations (figure 2). The N dislocations have the same orientation, perpendicular to \mathcal{L} and the same Burgers vectors \mathbf{b} . Possible interactions between dislocations are not considered, except in the term of mass, as

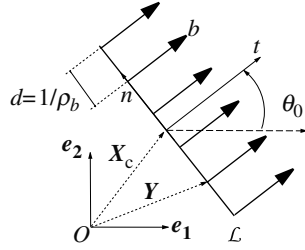


Figure 2. Grain boundary represented as a line \mathcal{L} , of length L and containing a density ρ_b of gliding edge dislocations with Burgers vector \mathbf{b} . \mathbf{X}_c denotes the centre of \mathcal{L} and \mathbf{Y} the position along \mathcal{L} . (\mathbf{t}, \mathbf{n}) is the basis associated with \mathcal{L} , making an angle $\theta_0 \equiv (\mathbf{e}_1, \mathbf{b})$.

discussed in §3c. The potential \mathbf{V}^{GB} associated with the grain boundary is obtained by summing over dislocations

$$\mathbf{V}^{\text{GB}}(\mathbf{x}) = \frac{\mu b^2}{m\omega^2} \rho_b \int_{\mathcal{L}} dX \mathbf{R}_{2\theta_0} \mathbf{J} \nabla \delta(\mathbf{x} - \mathbf{Y}) \nabla_{|\mathbf{Y}}^{\text{T}} \mathbf{R}_{2\theta_0} \mathbf{J}, \quad (2.8)$$

where $\mathbf{Y} = \mathbf{X}_c + \mathbf{X}$, with \mathbf{X}_c an origin point on \mathcal{L} and \mathbf{X} oriented along \mathcal{L} .

(c) Scattering functions of a single grain boundary

In this section, we derive the scattering functions for a single grain boundary in the first Born approximation. \mathbf{X}_c is set equal to $\mathbf{0}$ without loss of generality ($\mathbf{Y} = \mathbf{X}$).

Within the first Born approximation, the integral representation for the solution of equation (2.5) is

$$\mathbf{v}^s(\mathbf{x}) = \int d\mathbf{x}' \mathbf{G}^0(\mathbf{x} - \mathbf{x}', \omega) \mathbf{V}^{\text{GB}}(\mathbf{x}') \mathbf{v}^{\text{inc}}(\mathbf{x}'), \quad (2.9)$$

where \mathbf{V}^D has been replaced by the grain boundary potential \mathbf{V}^{GB} introduced in equation (2.8), and \mathbf{v} has been replaced in the right-hand side term by \mathbf{v}^{inc} (the velocity displacement of the incident wave). This assumes weak scattering since the total velocity $\mathbf{v} = \mathbf{v}^{\text{inc}} + \mathbf{v}^s$ is assumed to be equal to \mathbf{v}^{inc} at leading order (the wave scattered by the rest of the grain boundary on one dislocation is neglected).

In the case of polarized waves, one has to distinguish the amplitudes A_α and A_β of the longitudinal and transverse incident waves, respectively,

$$\mathbf{v}^{\text{inc}}(\mathbf{x}) = A_\alpha \mathbf{e}_1 e^{ik_\alpha x_1} + A_\beta \mathbf{e}_2 e^{ik_\beta x_1}. \quad (2.10)$$

The incident wave propagates along the \mathbf{e}_1 -axis, so that the velocity of the longitudinal wave is along \mathbf{e}_1 and the velocity of the transverse wave is along \mathbf{e}_2 (figure 3). In the following, $\mathbf{v}_\alpha^s(\mathbf{x})$ [$\mathbf{v}_\beta^s(\mathbf{x})$] denotes the solution of equations (2.9) and (2.10) with $A_\beta = 0$ ($A_\alpha = 0$, respectively).

Because equation (2.9) is linear, the full solution is simply the superposition $\mathbf{v}^s = \mathbf{v}_\alpha^s + \mathbf{v}_\beta^s$. We present in the following the detailed derivation of the scattered wave $\mathbf{v}_\alpha^s(\mathbf{x})$. The derivation of $\mathbf{v}_\beta^s(\mathbf{x})$ is performed in a similar way.

We first express the components of $\mathbf{v}_\alpha^s(\mathbf{x})$ (respectively, $\mathbf{v}_\beta^s(\mathbf{x})$) in cylindrical components: the first component corresponds to the projection of

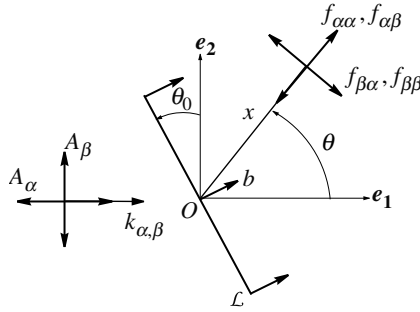


Figure 3. Scattering of an incident wave with longitudinal and transverse polarizations (A_α and A_β , respectively) by a grain boundary \mathcal{L} . At an observation angle θ and at large distances x from \mathcal{L} , the scattered field is composed of a longitudinal wave (with scattering functions $f_{\alpha\alpha}$ and $f_{\alpha\beta}$ because of mode conversion) and of a transverse wave (with scattering functions $f_{\beta\alpha}$ and $f_{\beta\beta}$).

$\mathbf{v}_\alpha^s(\mathbf{x})$ along the position vector \mathbf{x} , with $\theta \equiv (\widehat{\mathbf{e}_1, \mathbf{x}})$ and the second component is the azimuthal component. In this local basis, we use two remarkable properties: (i) the Green function $\tilde{\mathbf{G}}^0(x, \omega)$, defined by $\mathbf{G}_{ij}^0(\mathbf{x}, \omega) = \mathbf{R}_{\theta, ik} \tilde{\mathbf{G}}_{kl}^0(x, \omega) \mathbf{R}_{-\theta, lj}$, is diagonal and independent of θ (x denotes the magnitude of the position vector \mathbf{x}); (ii) the polar components of \mathbf{v}^s are directly related to the scattering functions $f_{\alpha\alpha}(\theta)$ and $f_{\beta\alpha}(\theta)$. In these notations, $f_{ab}(\theta)$ is the a -component of the scattered wave, for a given incident b -wave. That is, in the limit $kx \gg 1$,

$$\begin{pmatrix} v_{\alpha,t}^s \\ v_{\alpha,n}^s \end{pmatrix} = A_\alpha \begin{pmatrix} f_{\alpha\alpha}(\theta) \frac{e^{ik_\alpha x}}{\sqrt{x}} \\ f_{\beta\alpha}(\theta) \frac{e^{ik_\beta x}}{\sqrt{x}} \end{pmatrix}, \quad \text{resp.} \quad \begin{pmatrix} v_{\beta,t}^s \\ v_{\beta,n}^s \end{pmatrix} = A_\beta \begin{pmatrix} f_{\alpha\beta}(\theta) \frac{e^{ik_\alpha x}}{\sqrt{x}} \\ f_{\beta\beta}(\theta) \frac{e^{ik_\beta x}}{\sqrt{x}} \end{pmatrix}. \quad (2.11)$$

The scattering functions $f_{\beta\alpha}$ and $f_{\alpha\beta}$ quantify mode conversions, i.e. the transverse wave generated from scattering of a longitudinal incident wave, and vice versa.

Using equation (2.8) and setting $A_\beta = 0$, $A_\alpha = 1$, the integral representation (2.9) reads

$$\mathbf{v}_\alpha^s(\mathbf{x}) = \frac{\rho_b \mu b^2}{m\omega^2} \int d\mathbf{x}' \int_{\mathcal{L}} dX \mathbf{G}^0(\mathbf{x} - \mathbf{x}', \omega) \mathbf{R}_{2\theta_0} \mathbf{J} \nabla' \delta(\mathbf{x}' - \mathbf{X}) \nabla_{|\mathbf{X}}^T \mathbf{R}_{2\theta_0} \mathbf{J} \mathbf{e}_1 e^{ik_\alpha x'_1}. \quad (2.12)$$

In the integral above, we have

$$\nabla_{|\mathbf{X}}^T \mathbf{R}_{2\theta_0} \mathbf{J} \mathbf{e}_1 e^{ik_\alpha x'_1} = ik_\alpha \mathbf{e}_1^T \mathbf{R}_{2\theta_0} \mathbf{J} \mathbf{e}_1 e^{ik_\alpha X_1} = -ik_\alpha \sin 2\theta_0 e^{ik_\alpha X_1}, \quad (2.13)$$

and the integral over x' is

$$\left(\int d\mathbf{x}' \mathbf{G}^0(\mathbf{x} - \mathbf{x}', \omega) \mathbf{R}_{2\theta_0} \mathbf{J} \nabla' \delta(\mathbf{x}' - \mathbf{X}) \right)^T = \nabla^T \mathbf{R}_{2\theta_0} \mathbf{J} \mathbf{G}^0(\mathbf{x} - \mathbf{X}, \omega). \quad (2.14)$$

We now use, for $x \gg X$ (x, X denote the magnitude of the position vectors \mathbf{x}, \mathbf{X}), the asymptotic form of Green's function in two-dimensional free space,

$$G^0(\mathbf{x} - \mathbf{X}, \omega) \xrightarrow{x \rightarrow \infty} \frac{e^{i\pi/4}}{2\sqrt{2\pi x}} \mathbf{R}_\theta \begin{pmatrix} \frac{e^{ik_\alpha[x+X \sin(\theta_0-\theta)]}}{\sqrt{k_\alpha} \gamma^2} & 0 \\ 0 & \frac{e^{ik_\beta[x+X \sin(\theta_0-\theta)]}}{\sqrt{k_\beta}} \end{pmatrix} \mathbf{R}_{-\theta}. \quad (2.15)$$

We have used $\mathbf{X} = X \mathbf{R}_{\theta_0} \mathbf{e}_2$: with $\mathbf{X}_c = 0$, \mathbf{X} is along the direction of the dislocation line, perpendicular to the Burgers vector (\mathbf{b} is along $\mathbf{R}_{\theta_0} \mathbf{e}_1$).

In general, $\nabla = \partial_x (\mathbf{R}_\theta \mathbf{e}_1) + (1/x) \partial_\theta (\mathbf{R}_\theta \mathbf{e}_2)$. At leading order in x , the terms coming from the derivation with respect to θ can be neglected, so that we formally write $\nabla = \mathbf{R}_\theta \partial_x \mathbf{e}_1$ that involves the leading order terms. We get for the cylindrical components

$$\begin{pmatrix} \mathbf{v}_{\alpha,t}^s(\mathbf{x}) \\ \mathbf{v}_{\alpha,n}^s(\mathbf{x}) \end{pmatrix} = \mathbf{R}_{-\theta} \begin{pmatrix} \mathbf{v}_{\alpha,1}^s(\mathbf{x}) \\ \mathbf{v}_{\alpha,2}^s(\mathbf{x}) \end{pmatrix} \\ = \frac{\rho_b \mu b^2}{m\omega^2} \frac{e^{i\pi/4}}{2\sqrt{2\pi|x|}} \sin 2\theta_0 k_\alpha \int_{\mathcal{L}} dX e^{ik_\alpha X_1} \begin{pmatrix} \frac{\sqrt{k_\alpha}}{\gamma^2} e^{ik_\alpha[x+X \sin(\theta_0-\theta)]} \sin 2(\theta - \theta_0) \\ \sqrt{k_\beta} e^{ik_\beta[x+X \sin(\theta_0-\theta)]} \cos 2(\theta - \theta_0) \end{pmatrix},$$

where we have used $\mathbf{R}_{2\theta_0-\theta} \mathbf{J} \mathbf{R}_\theta \mathbf{e}_1 = \begin{pmatrix} \sin 2(\theta - \theta_0) \\ \cos 2(\theta - \theta_0) \end{pmatrix}$. We finally obtain

$$\begin{pmatrix} \mathbf{v}_{\alpha,t}^s(\mathbf{x}) \\ \mathbf{v}_{\alpha,n}^s(\mathbf{x}) \end{pmatrix} = \frac{\mu N b^2}{m\omega^2} \frac{e^{i\pi/4}}{2\sqrt{2\pi x}} \sin 2\theta_0 k_\alpha \\ \times \begin{pmatrix} \frac{\sqrt{k_\alpha}}{\gamma^2} e^{ik_\alpha x} \text{sinc}\{k_\alpha L/2[\sin(\theta_0 - \theta) - \sin \theta_0]\} \sin 2(\theta - \theta_0) \\ \sqrt{k_\beta} e^{ik_\beta x} \text{sinc}\{k_\beta L/2[\sin(\theta_0 - \theta) - \sin \theta_0/\gamma]\} \cos 2(\theta - \theta_0) \end{pmatrix}. \quad (2.16)$$

The case of the transverse incident wave can be treated using the same route as in §2a: In equation (2.12), the term $\nabla_{|\mathbf{X}}^{\prime T} \mathbf{R}_{2\theta_0} \mathbf{J} \mathbf{e}_1 e^{ik_\alpha x'_1} = -ik_\alpha \sin 2\theta_0 e^{ik_\alpha X_1}$ has to be replaced by $\nabla_{|\mathbf{X}}^{\prime T} \mathbf{R}_{2\theta_0} \mathbf{J} \mathbf{e}_2 e^{ik_\beta x'_1} = ik_\beta \cos 2\theta_0 e^{ik_\beta X_1}$. We deduce

$$\begin{pmatrix} \mathbf{v}_{\beta,t}^s(\mathbf{x}) \\ \mathbf{v}_{\beta,n}^s(\mathbf{x}) \end{pmatrix} = -\frac{\mu N b^2}{m\omega^2} \frac{e^{i\pi/4}}{2\sqrt{2\pi x}} \cos 2\theta_0 k_\beta \\ \times \begin{pmatrix} \frac{\sqrt{k_\alpha}}{\gamma^2} e^{ik_\alpha x} \text{sinc}\{k_\alpha L/2[\sin(\theta_0 - \theta) - \gamma \sin \theta_0]\} \sin 2(\theta - \theta_0) \\ \sqrt{k_\beta} e^{ik_\beta x} \text{sinc}[k_\beta L/2(\sin(\theta_0 - \theta) - \sin \theta_0)] \cos 2(\theta - \theta_0) \end{pmatrix}. \quad (2.17)$$

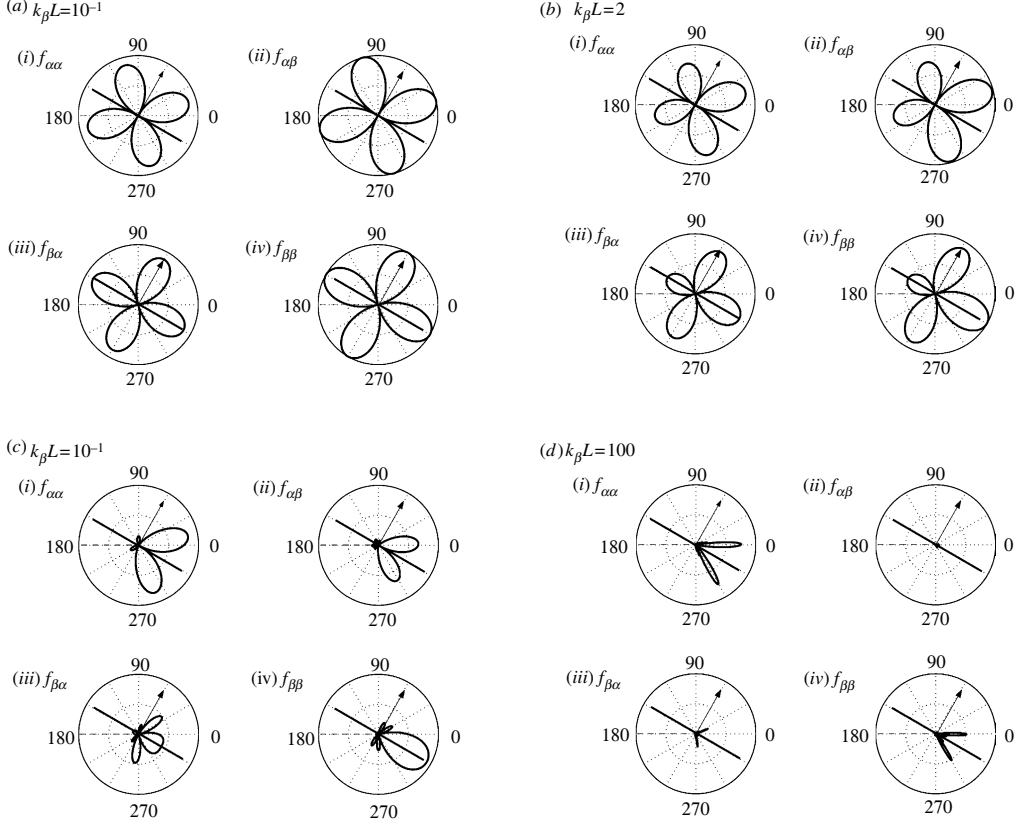


Figure 4. Scattering functions of a grain boundary (in plain lines). The direction of the Burgers vector is indicated by the arrow, the incident wave has the direction $\theta=0$.

The scattering functions are then written by identifying equations (2.16) and (2.17) with equation (2.11),

$$\left. \begin{aligned}
 f_{\alpha\alpha}(\theta) &= \frac{\mu N b^2}{m \omega^2} \frac{k_\alpha^3}{2\sqrt{2\pi}\gamma^2} \sin 2\theta_0 \sin 2(\theta - \theta_0) \operatorname{sinc}[k_\alpha L/2(\sin(\theta_0 - \theta) - \sin \theta_0)] e^{i\pi/4}, \\
 f_{\beta\alpha}(\theta) &= \frac{\mu N b^2}{m \omega^2} \frac{k_\alpha k_\beta^{1/2}}{2\sqrt{2\pi}\gamma^2} \sin 2\theta_0 \cos 2(\theta - \theta_0) \operatorname{sinc}[k_\beta L/2(\sin(\theta_0 - \theta) - \sin \theta_0/\gamma)] e^{i\pi/4}, \\
 f_{\alpha\beta}(\theta) &= -\frac{\mu N b^2}{m \omega^2} \frac{k_\beta k_\alpha^{1/2}}{2\sqrt{2\pi}} \cos 2\theta_0 \sin 2(\theta - \theta_0) \operatorname{sinc}[k_\alpha L/2(\sin(\theta_0 - \theta) - \gamma \sin \theta_0)] e^{i\pi/4}, \\
 f_{\beta\beta}(\theta) &= -\frac{\mu N b^2}{m \omega^2} \frac{k_\beta^3}{2\sqrt{2\pi}} \cos 2\theta_0 \cos 2(\theta - \theta_0) \operatorname{sinc}[k_\beta L/2(\sin(\theta_0 - \theta) - \sin \theta_0)] e^{i\pi/4}.
 \end{aligned} \right\} \quad (2.18)$$

The polar plots of the scattering functions are shown in [figure 4](#). As expected, for wavelengths large compared to L , the scattering functions tend to those

obtained for a single dislocation with Burgers vector $\mathbf{B} \equiv Nb$ and mass $M \equiv Nm$ (see Maurel *et al.* 2004a).

3. The multiple scattering mechanism for the modified Green function

(a) Principle of the calculation

The multiple scattering formalism we use is based on the calculation of the modified Green function $\langle \mathbf{G} \rangle(\mathbf{k})$ with \mathbf{k} the wavevector that comes from the Fourier transform of $G(\mathbf{x})$. The modified Green function describes the elastic medium filled with scatterers randomly distributed (here, the segments \mathcal{L} representing grain boundaries) in terms of an effective medium. The averaging process over disorder realizations involves averages over the lengths L of the segments, over the dislocations densities $\rho_b = 1/d$ held by each segment (d denotes the distance between two dislocations), over the Burgers vectors \mathbf{b} of the $N = \rho_b L$ dislocations held by the segments, and over the positions and orientations of the segments (\mathbf{X}_c, θ_0) (figure 2). The modified Green function is given by the Dyson equation (see, for instance, Sheng 1995),

$$\langle G \rangle(\mathbf{k}) = \left[\mathbf{G}^{0^{-1}}(\mathbf{k}) - \Sigma(\mathbf{k}) \right]^{-1}, \quad (3.1)$$

where \mathbf{G}^0 is the free space Green function and $\Sigma(\mathbf{k})$ the so-called mass operator. When the properties of the coherent wave differ little from the waves in the homogeneous medium, $\Sigma(\mathbf{k})$ can be perturbatively expanded in powers of a small parameter ϵ (for a discussion/definition of ϵ , see §3c): $\Sigma(\mathbf{k}) = \Sigma_1(\mathbf{k}) + \Sigma_2(\mathbf{k}) + \dots$. In the present case, we need to compute at least the first two terms, because the imaginary part of the leading term $\Sigma_1(\mathbf{k})$ vanishes. These terms are given by

$$\left. \begin{aligned} \Sigma_1(\mathbf{k}) &= n \int d\mathbf{x} d\mathbf{C} e^{-i\mathbf{k} \cdot \mathbf{x}} \mathbf{V}^{\text{GB}}(\mathbf{x}) e^{i\mathbf{k} \cdot \mathbf{x}}, \\ \Sigma_2(\mathbf{k}) &= n \int d\mathbf{x} d\mathbf{x}' d\mathbf{C} e^{-i\mathbf{k} \cdot \mathbf{x}} \mathbf{V}^{\text{GB}}(\mathbf{x}) \mathbf{G}^0(\mathbf{x} - \mathbf{x}') \mathbf{V}^{\text{GB}}(\mathbf{x}') e^{i\mathbf{k} \cdot \mathbf{x}'}, \end{aligned} \right\} \quad (3.2)$$

where n denotes the number density of scatterers (grain boundaries) per unit area and the integral over \mathbf{C} corresponds to averages over all relevant parameters. Here, $d\mathbf{C} = p(b)dbp(L)dLp(\rho_b)d\rho_b(d\mathbf{X}_c/\mathcal{V})(d\theta_0/2\pi)$, where $p(X)$ denotes the probability distribution function of the quantity X (in the following, we note $\langle X \rangle = \int dX X p(X)$). In equation (3.2), we have assumed that the scatterers are not spatially correlated.

The (complex) poles of $\langle G \rangle(\mathbf{k})$ give the wavenumbers K_α and K_β of the coherent waves that can propagate in the effective medium. Their real part is related to the index of refraction whereas their imaginary part is related to the attenuation length.

We report in §3b the derivation of $\Sigma(\mathbf{k})$ at order 1. The derivation at order 2, that involves similar calculations, is detailed in electronic supplementary material-3.

(b) Derivation of the mass operator

(i) Order 1

We start from the expression (3.2) for $\Sigma_1(\mathbf{k})$,

$$\Sigma_1(\mathbf{k}) = n \int d\mathbf{x} p(b)p(L)p(d\rho_b)db dL d\rho_b \frac{d\theta_0}{2\pi} \frac{d\mathbf{X}_c}{\mathcal{V}} e^{-i\mathbf{k}\cdot\mathbf{x}} \mathbf{V}^{\text{GB}}(\mathbf{x}) e^{i\mathbf{k}\cdot\mathbf{x}}. \quad (3.3)$$

Using equation (2.8), we get

$$\begin{aligned} \Sigma_1(\mathbf{k}) &= n \frac{\mu}{\omega^2} \left\langle \frac{\rho_b b^2}{m} \right\rangle \int d\mathbf{x} p(L) dL \frac{d\theta_0}{2\pi} \frac{d\mathbf{X}_c}{\mathcal{V}} \\ &\quad \times \int_{\mathcal{L}} dX e^{-i\mathbf{k}\cdot\mathbf{x}} \mathbf{R}_{2\theta_0} \mathbf{J} \nabla \delta(\mathbf{x} - \mathbf{Y}) \nabla_{|\mathbf{Y}}^T \mathbf{R}_{2\theta_0} \mathbf{J} e^{i\mathbf{k}\cdot\mathbf{x}}. \end{aligned}$$

By using $\nabla_{|\mathbf{Y}}^T e^{i\mathbf{k}\cdot\mathbf{x}} = i\mathbf{k}^T e^{i\mathbf{k}\cdot\mathbf{Y}}$ and integrating by part $\int d\mathbf{x} e^{-i\mathbf{k}\cdot\mathbf{x}} \nabla \delta(\mathbf{x} - \mathbf{Y}) = i\mathbf{k} e^{-i\mathbf{k}\cdot\mathbf{Y}}$, we obtain

$$\begin{aligned} \Sigma_1(\mathbf{k}) &= -n \frac{\mu}{\omega^2} \left\langle \frac{\rho_b b^2}{m} \right\rangle \int p(L) dL \frac{d\theta_0}{2\pi} \frac{d\mathbf{X}_c}{\mathcal{V}} \int_{\mathcal{L}} dX \mathbf{R}_{2\theta_0} \mathbf{J} \mathbf{k}^T \mathbf{k} \mathbf{R}_{2\theta_0} \mathbf{J} \\ &= -n \frac{\mu}{\omega^2} \left\langle \frac{\rho_b L b^2}{m} \right\rangle \int \frac{d\theta_0}{2\pi} \mathbf{R}_{2\theta_0} \mathbf{J} \mathbf{k}^T \mathbf{k} \mathbf{R}_{2\theta_0} \mathbf{J}. \end{aligned} \quad (3.4)$$

We now focus on the matrix $\mathbf{R}_{2\theta_0} \mathbf{J} \mathbf{k}^T \mathbf{k} \mathbf{R}_{2\theta_0} \mathbf{J}$ whose average over θ_0 has to be taken. With $\mathbf{k} = k \mathbf{R}_{\xi} \mathbf{e}_1$ (i.e. $\xi \equiv \widehat{(\mathbf{e}_1, \mathbf{k})}$), and using $\mathbf{P}_1 \equiv \mathbf{e}_1^T \mathbf{e}_1$ and $\mathbf{P}_2 \equiv \mathbf{e}_2^T \mathbf{e}_2 = \mathbf{J} \mathbf{P}_1 \mathbf{J}$, it is easy to see that $\mathbf{R}_{2\theta_0} \mathbf{J} \mathbf{k}^T \mathbf{k} \mathbf{R}_{2\theta_0} \mathbf{J} = k^2 \mathbf{R}_{(2\theta_0-\xi)} \mathbf{P}_2 \mathbf{R}_{-(2\theta_0-\xi)}$. Changing the variable $\theta_0 \rightarrow \theta_0 - \xi/2$, we obtain

$$\begin{aligned} \Sigma_1(\mathbf{k}) &= -\frac{\mu n}{2\pi\omega^2} \left\langle \frac{N b^2}{m} \right\rangle k^2 \int d\theta_0 \mathbf{R}_{2\theta_0} \mathbf{P}_2 \mathbf{R}_{-2\theta_0} \\ &= -\frac{\mu n}{2\omega^2} \left\langle \frac{N b^2}{m} \right\rangle k^2 \begin{pmatrix} 1 & 0 \\ 0 & 1 \end{pmatrix}. \end{aligned} \quad (3.5)$$

For a single grain boundary, the total Burgers vector is $\mathbf{B} \equiv N b$ and the total mass is $M \equiv N m$. Expression (3.5) is actually the same as obtained for a random distribution of isolated dislocations of Burgers vector \mathbf{B} and mass M (Maurel *et al.* 2004b),

$$\Sigma_1(\mathbf{k}) = -\frac{1}{2} \frac{\mu n}{\omega^2} \left\langle \frac{B^2}{M} \right\rangle k^2 \begin{pmatrix} 1 & 0 \\ 0 & 1 \end{pmatrix}. \quad (3.6)$$

This result shows that there is no effect of the line distribution of dislocations along the segments \mathcal{L} at this order: grain boundaries are seen as spatially uncorrelated ('fat') single dislocations.

(ii) *Order 2*

The calculation of $\Sigma_2(\mathbf{k})$ is similar to that presented earlier and is detailed in the electronic supplementary material-3. We obtain

$$\Sigma_2(k) = \frac{i}{16} \left(\frac{\mu n}{\omega^2} \right)^2 \left\langle \frac{N^2 b^4}{m^2} \right\rangle \frac{1 + \gamma^4}{\gamma^4} \frac{k_\beta^2}{n} k^2 \mathbf{R}_\xi \begin{pmatrix} I_1(kL) & 0 \\ 0 & I_2(kL) \end{pmatrix} \mathbf{R}_{-\xi}, \quad (3.7)$$

with

$$I_1(kL) = \frac{1}{\pi^2 \langle L^2 \rangle (1 + \gamma^4)} \int p(L) L^2 dL d\theta_0 d\zeta \sin^2 2\theta_0 \\ \times \{ \cos^2 2\zeta f(k_\alpha L, kL, \theta_0, \zeta) + \gamma^4 \sin^2 2\zeta f(k_\beta L, kL, \theta_0, \zeta) \},$$

$$I_2(kL) = \frac{1}{\pi^2 \langle L^2 \rangle (1 + \gamma^4)} \int p(L) L^2 dL d\theta_0 d\zeta \cos^2 2\theta_0 \\ \times \{ \cos^2 2\zeta f(k_\alpha L, kL, \theta_0, \zeta) + \gamma^4 \sin^2 2\zeta f(k_\beta L, kL, \theta_0, \zeta) \},$$

and

$$f(qL, kL, \theta_0, \zeta) = \text{sinc}^2[(k \sin \theta_0 - q \sin \zeta)L/2],$$

where $\text{sinc}(x) \equiv \sin(x)/x$. It is easy to see that $I_{a=1,2}$ goes to unity as kL tends to zero. Hence, the limit of expression (3.7) at long wavelengths is the same as that obtained for a random distribution of single dislocations of Burgers vector \mathbf{B} and mass M ,

$$\Sigma_2(k) = \frac{i}{16} \left(\frac{\mu n}{\omega^2} \right)^2 \left\langle \frac{B^4}{M^2} \right\rangle \frac{1 + \gamma^4}{\gamma^4} \frac{k_\beta^2}{n} k^2 \begin{pmatrix} 1 & 0 \\ 0 & 1 \end{pmatrix}. \quad (3.8)$$

Using

$$G^0(\mathbf{k}) = \mathbf{R}_\xi \begin{pmatrix} \gamma^2(k^2 - k_\alpha^2) & 0 \\ 0 & (k^2 - k_\beta^2) \end{pmatrix} \mathbf{R}_{-\xi}, \quad (3.9)$$

the modified Green function finally reads

$$\langle G \rangle^{-1}(\mathbf{k}) = \mathbf{R}_\xi \left[\begin{pmatrix} \gamma^2(k^2 - k_\alpha^2) & 0 \\ 0 & k^2 - k_\beta^2 \end{pmatrix} + \frac{1}{2} \frac{\mu n}{\omega^2} \left\langle \frac{B^2}{M} \right\rangle k^2 \begin{pmatrix} 1 & 0 \\ 0 & 1 \end{pmatrix} \right. \\ \left. - \frac{i}{16} \left(\frac{\mu n}{\omega^2} \right)^2 \left\langle \frac{N^2 b^4}{m^2} \right\rangle \frac{1 + \gamma^4}{\gamma^4} \frac{k_\beta^2}{n} k^2 \begin{pmatrix} I_1(kL) & 0 \\ 0 & I_2(kL) \end{pmatrix} \right] \mathbf{R}_{-\xi}. \quad (3.10)$$

(c) *Discussion*

Let us comment on expression (3.10). For the sake of clarity, we take all grain boundaries with the same number of dislocations, so that $N^2 = \langle N \rangle^2 = \langle N^2 \rangle$.

Relation (2.4) can be written as $m \simeq \rho b^2 / \epsilon$, where $\epsilon \equiv 1 / \ln(\delta / \delta_0)$ is the small parameter in multiple scattering by single dislocations. We have $B^2 / M \simeq N\epsilon / \rho$ and we define

$$\epsilon' \equiv \frac{n}{k_\beta^2}, \quad (3.11)$$

so that we can write, for $\mathbf{k} = k\mathbf{e}_1$ (i.e. $\xi = 0$),

$$\begin{aligned} \langle G \rangle^{-1}(k) &= \mathbf{G}^{0^{-1}}(k) \\ &+ \epsilon' k^2 \left[\frac{1}{2} N\epsilon \begin{pmatrix} 1 & 0 \\ 0 & 1 \end{pmatrix} - \frac{i}{16} \frac{1 + \gamma^4}{\gamma^4} (N\epsilon)^2 \begin{pmatrix} I_1(kL) & 0 \\ 0 & I_2(kL) \end{pmatrix} \right]. \end{aligned} \quad (3.12)$$

The weak scattering limit corresponds to

- (i) ϵ' finite, that is no vanishing value of $k_\beta L_c$, with $L_c \simeq 1 / \sqrt{n}$;
- (ii) $N\epsilon \ll 1$, with $\epsilon \simeq 1 / \ln(\delta / \delta_0)$.

The first condition introduces a cut-off length L_c for the ultrasonic wavelength that can be used. As the interaction strength between the wave and a dislocation increases with increasing wavelength, this condition corresponds to a non-divergence of the scattering strength. This condition introduces a characteristic length that is relevant in the forthcoming expressions of the refraction indices (4.2) and of the attenuation lengths (4.4). Note that in a recent experiment (Zolotoyabko *et al.* 2001; Shilo & Zolotoyabko 2002, 2003), high-frequency ultrasonic waves have been used in a LiNbO₃ crystal, corresponding to $k_\beta L_c \simeq 10$, thus fulfilling condition (i).

Condition (ii) involves properties of the medium itself. For an isolated dislocation, the long cut-off length δ is given by the size of the sample and the short cut-off length $\delta_0 \simeq b$. In grain boundaries, the upper cut-off length δ can be chosen as the distance d between dislocations (Shockley & Read 1949). For a tilt boundary, L , N and b are linked through $L = Nd$, with $d = b / \theta_b$ and θ_b the (small) misorientation angle. We thus obtain the condition

$$N\epsilon = \frac{(L/b)}{\ln(d/b)} \theta_b \ll 1.$$

With $L \gg b$, this condition gives a restriction on the angle θ_b of the grain boundary.

4. Characteristics of the coherent waves

The wavenumbers K_α and K_β of the coherent longitudinal and transverse waves, respectively, are given by the poles of $\langle G \rangle(k)$. In equation (3.10), the first diagonal term of $\langle G \rangle^{-1}(k)$ gives the longitudinal wave (directed along \mathbf{k}); the second diagonal term yields the transverse wave, in the direction perpendicular to \mathbf{k} . In the weak scattering approximation, K_α is expected to be close to k_α (and K_β close to k_β). In equation (3.10), we thus replace $I_1(kL)$ by

$I_1(k_\alpha L)$ (and $I_2(kL)$ by $I_2(k_\beta L)$). Thus, the coherent wavenumbers read

$$\left. \begin{aligned} K_\alpha &= k_\alpha \left[1 - \frac{1}{4\gamma^2} \frac{\mu n}{\omega^2} \left\langle \frac{Nb^2}{m} \right\rangle + i \frac{1 + \gamma^4}{32\gamma^4} \left(\frac{\mu n}{\omega^2} \right)^2 \left\langle \frac{N^2 b^4}{m^2} \right\rangle \frac{k_\alpha^2}{n} I_1(k_\alpha L) \right], \\ K_\beta &= k_\beta \left[1 - \frac{1}{4} \frac{\mu n}{\omega^2} \left\langle \frac{Nb^2}{m} \right\rangle + i \frac{1 + \gamma^4}{32\gamma^4} \left(\frac{\mu n}{\omega^2} \right)^2 \left\langle \frac{N^2 b^4}{m^2} \right\rangle \frac{k_\beta^2}{n} I_2(k_\beta L) \right]. \end{aligned} \right\} \quad (4.1)$$

At first-order, this expression reduces to the results obtained following Foldy's approach (see §4c).

(a) *Index of refraction and attenuation length*

We define the index of refraction as $n_\alpha \equiv \alpha/V_\alpha$ (respectively, $n_\beta \equiv \beta/V_\beta$), where $V_a = \text{Re}(\omega/K_a)$ denote the phase velocities in the presence of grain boundaries (recall that α and β are the phase velocities in the absence of grain boundaries). From equation (4.1), we obtain

$$\left. \begin{aligned} n_\alpha &= 1 - \frac{1}{4\gamma^2} \frac{\mu n}{\omega^2} \left\langle \frac{Nb^2}{m} \right\rangle, \\ n_\beta &= 1 - \frac{1}{4} \frac{\mu n}{\omega^2} \left\langle \frac{Nb^2}{m} \right\rangle. \end{aligned} \right\} \quad (4.2)$$

As observed for a distribution of isolated dislocations (Maurel *et al.* 2004b):

- (i) the effective phase velocity is larger than its value in the absence of scatterers. The group velocity is however smaller;
- (ii) the index of refraction decreases with increasing wavelength.

As first observed by Nabarro (1951) and confirmed in our calculations, this result is due to the particular interaction between an elastic wave and a dislocation (e.g. in equation (2.3)). The scattering waves actually occur from the motion of the dislocation driven by the incident wave. The equation of motion (Lund 1988) shows that the amplitude of dislocation motion increases with increasing wavelengths, which also increases the scattered energy. Of course, no divergence of the index occurs since the difference of $n_{\alpha,\beta}$ to unity is of order $N\epsilon\epsilon'$. With the condition that ϵ' remains finite, values of wavelengths have an upper limit given by the cut-off length L_c . By considering identical grain boundaries, equation (4.2) reads

$$\left. \begin{aligned} n_\alpha &= 1 - \frac{1}{4\gamma^2} \frac{\mu n B^2}{M\omega^2} = 1 - \frac{1}{4\gamma^4} \frac{N\epsilon}{(k_\alpha L_c)^2}, \\ n_\beta &= 1 - \frac{1}{4} \frac{\mu n B^2}{M\omega^2} = 1 - \frac{1}{4} \frac{N\epsilon}{(k_\beta L_c)^2}. \end{aligned} \right\} \quad (4.3)$$

(b) *Attenuation lengths*

The attenuation length \mathcal{L}_a is given by the imaginary part of the wavenumber: $\mathcal{L}_a \equiv 1/\text{Im}(K_a)$. It corresponds to the loss of coherence due to scattering away

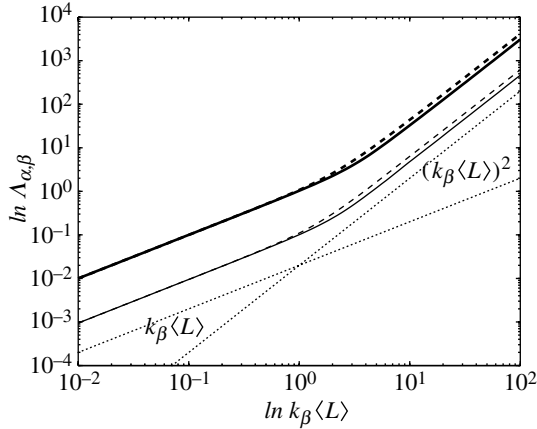


Figure 5. Variations of A_α, A_β (with $\gamma=1.4$) as a function of $k_\beta \langle L \rangle$. The bold lines represent A_α , with a grain boundary length distribution given by $p(L) \propto \delta(L - \langle L \rangle)$ (solid line) and $p(L) = 1/(2\langle L \rangle)$ (dashed line). The thin lines represent A_β , with the same notations. The straight dashed lines are guides to the eye.

from the forward direction. From equation (4.1), we obtain

$$\left. \begin{aligned} A_\alpha &= \frac{32\gamma^4}{1 + \gamma^4} \frac{\alpha^4}{n\mu^2} \left\langle \frac{m^2}{N^2 b^4} \right\rangle \frac{k_\alpha}{I_1(k_\alpha L)} \sim \frac{32\gamma^8}{1 + \gamma^4} \frac{1}{(N\epsilon)^2} \frac{k_\alpha L_c}{I_1(k_\alpha L)} L_c, \\ A_\beta &= \frac{32\gamma^4}{1 + \gamma^4} \frac{\beta^4}{n\mu^2} \left\langle \frac{m^2}{N^2 b^4} \right\rangle \frac{k_\beta}{I_2(k_\beta L)} \sim \frac{32\gamma^4}{1 + \gamma^4} \frac{1}{(N\epsilon)^2} \frac{k_\beta L_c}{I_2(k_\beta L)} L_c, \end{aligned} \right\} \quad (4.4)$$

where the symbol ‘ \sim ’ can be replaced by an equality if all grain boundaries are identical. The attenuation lengths are plotted in figure 5 as a function of wavenumber. Note the presence of a linear and a quadratic regime, with a cross-over between both behaviours occurring at wavenumbers of the order of the average grain boundary length. The linear regime coincides with the results obtained with single dislocations (Maurel *et al.* 2004b) with the total Burgers vector \mathbf{B} and the total mass M . Increasing the wavelength decreases the attenuation length $A_{\alpha,\beta}$, an unusual behaviour for waves propagating in random media. Conversely, waves do not attenuate at very small wavenumbers (as the refraction index tends to one), a limit where the medium looks to be disorder-free. Recall that the expressions in equation (4.4) are not valid for large wavenumbers because of the condition that ϵ' remains finite.

Note also that, in the calculation presented here, the internal damping has been neglected in the equation of motion. Sources of dislocation damping can be multiple (Nabarro 1987), and are important at low frequencies. In spite of this limitation, the predictions discussed earlier could be further tested experimentally in a frequency range where damping forces are still small.

(c) Remark on the Foldy approach

An adaptation of the Foldy approach (Foldy 1945) can be found in Maurel *et al.* (2004b) for two-dimensional polarized waves. It was found, for an ensemble

of isolated dislocations, that $\langle f_{\alpha\beta} \rangle_{\mathbf{C}}(0) = \langle f_{\beta\alpha} \rangle_{\mathbf{C}}(0) = 0$ (in that case, we had $\mathbf{C} = (b, \theta_0)$). This property, that is the averaged cross-coupled scattered waves vanish, is also verified for the present case. Indeed, it can be seen from equation (2.18) that the average over θ_0 makes $\langle f_{\alpha,\beta} \rangle_{\mathbf{C}}(\theta)$ and $\langle f_{\beta,\alpha} \rangle_{\mathbf{C}}(\theta)$ (here, we have $\mathbf{C} = (b, L, \rho_b, \mathbf{X}_c, \theta_0)$) vanish at $\theta=0$.

Thus, the effective wavenumber K_a , with $a = \alpha, \beta$, can be written as a function of the averaged scattering functions

$$K_a = k_a + n \sqrt{\frac{2\pi}{k_a} \langle f_{aa} \rangle_{\mathbf{C}}(0)} e^{-i\pi/4}. \quad (4.5)$$

This relation leads to the same value for the modified wavenumber as in equation (4.1) at first-order. This is because the scattering functions have been calculated in the first Born approximation.

5. Concluding remarks

We have derived the dispersion relation of a two-dimensional continuous elastic medium filled with gliding edge dislocation arrays randomly distributed and oriented in space. It has been found that sound attenuation increases with wavelength, an effect probably due to the two-dimensional nature of the problem.

The present analysis is aimed to evaluate the plastic contribution to the multiple scattering of elastic waves that propagate through polycrystals and it is the first time, to the best of our knowledge, that the structure at the grain boundary is considered. Most of the studies have considered the variations between grains in the elastic constants, and mainly the change in anisotropy, as the source of scattering. Both effects may superpose in polycrystals, so including possible contribution of the dislocations could be helpful to obtain a better modelling of sound propagation in polycrystals.

This work was supported by the Consejo Nacional de Ciencia y Tecnología (CONACYT, Mexico) grant number 40867-F, by the CNRS/CONICYT in the framework of a French/Chilean collaboration on ‘Propagation of wave in continuous disordered media’ and by FONDAP grant no. 11980002.

References

- Eshelby, J. D. 1949 Dislocation as a cause of mechanical damping in metals. *Proc. R. Soc. A* **197**, 396–416.
- Eshelby, J. D. 1953 The equation of motion of a dislocation. *Phys. Rev.* **90**, 248–255.
- Foldy, L. L. 1945 The multiple scattering of waves. I. General theory of isotropic scattering by randomly distributed scatterers. *Phys. Rev.* **67**, 107–119.
- Granato, A. V. & Lücke, K. 1956a Theory of mechanical damping due to dislocations. *J. Appl. Phys.* **27**, 583–593.
- Granato, A. V. & Lücke, K. 1956b Application of dislocation theory to internal friction phenomena at high frequencies. *J. Appl. Phys.* **27**, 789–805.
- Granato, A. V. & Lücke, K. 1966 *Physical acoustics*, vol. 4A (ed. W. P. Mason). New York: Academic Press.

Elastic wave propagation in polycrystals

- Granato, A. V. & Lücker, K. 1981 Simplified theory of dislocation damping including point-defect drag. II. Superposition of continuous and pinning-point-drag effects. *Phys. Rev. B* **24**, 1017–7007.
- Hirsehorn, S. 1982 The scattering of ultrasonic waves by polycrystals. *J. Acoust. Soc. Am.* **72**, 1021–1231.
- Lifshitz, I. M. & Parkhomovskii, G. D. 1950 On the theory of the propagation of supersonic waves in polycrystals. *Z. Exsperim. Theor. Fiz.* **20**, 175–182.
- Lücker, K. & Granato, A. V. 1981 Simplified theory of dislocation damping including point-defect drag. I. Theory of drag by equidistant point defects. *Phys. Rev. B* **24**, 6991–7006.
- Lund, F. 1988 Response of a stringlike dislocation loop to an external stress. *J. Mater. Res.* **3**, 280–297.
- Lund, F. 2002 Sound–vortex interaction in infinite media. In *Sound flow interaction* (ed. Y. Aurégan *et al.*), pp. 112–160. Berlin: Springer.
- Maurel, A., Mercier, J.-F. & Lund, F. 2004a Scattering of an elastic wave by a single dislocation. *J. Acoust. Soc. Am.* **115**, 2773–2780.
- Maurel, A., Mercier, J.-F. & Lund, F. 2004b Elastic wave propagation through a random array of dislocations. *Phys. Rev. B* **70**, 024303.
- Mura, T. 1963 Continuous distribution of moving dislocations. *Phil. Mag.* **8**, 843–857.
- Nabarro, F. R. N. 1951 The interaction of screw dislocations and sound wave. *Proc. R. Soc. A.* **209**, 278–290.
- Nabarro, F. R. N. 1987 *Theory of crystal dislocations*. New York: Dover.
- Peach, M. O. & Koehler, J. S. 1950 The forces exerted on dislocations and the stress fields produced by them. *Phys. Rev.* **80**, 436–439.
- Rokhlin, S. I., Bolland, T. K. & Adler, L. 1991 High-frequency ultrasonic wave propagation in polycrystalline materials. *J. Acoust. Soc. Am.* **91**, 151–165.
- Sheng, P. 1995 *Introduction to wave scattering, localization, and mesoscopic phenomena*. New York: Academic Press.
- Shilo, D. & Zolotoyabko, E. 2002 Visualization of surface acoustic wave scattering by dislocations. *Ultrasonics* **40**, 921–925.
- Shilo, D. & Zolotoyabko, E. 2003 Visualization of short surface acoustic waves by stroboscopic x-ray topography: analysis of contrast. *J. Phys. D* **36**, A122–A127.
- Shockley, W. & Read, W. T. 1949 Quantitative predictions from dislocation models of crystal grain boundaries. *Phys. Rev.* **75**, 692.
- Stanke, F. E. & Kino, G. S. 1984 A unified theory for elastic wave propagation in polycrystalline materials. *J. Acoust. Soc. Am.* **75**, 665–681.
- Thompson, B. R. 2002 Elastic-wave propagation in random polycrystals: fundamentals and applications to nondestructive evaluation. *Imaging of complex media with acoustic and seismic waves*, vol. 84 (ed. Fink *et al.*), *Topics in applied physics*, pp. 233–256. Berlin: Springer.
- Zhang, G., Simpson Jr, W. A., Vitek, J. M., Barnard, D. J., Tweed, L. J. & Foley, J. 2004 Ultrasonic attenuation due to grain boundary scattering in copper and copper–aluminium. *J. Acoust. Soc. Am.* **116**, 109–116.
- Zolotoyabko, E., Shilo, D. & Lakin, E. 2001 X-ray imaging of acoustic wave interaction with dislocations. *Mater. Sci. Eng. A* **309–310**, 23–27.